Supplementary Material for: Dynamic dissipative cooling of a mechanical oscillator in strong-coupling optomechanics

Yong-Chun Liu[1,2], Yun-Feng Xiao[1],* Xingsheng Luan[2], and Chee Wei Wong[2†]
[1]*State Key Laboratory for Mesoscopic Physics and School of Physics, Peking University, Beijing 100871, P. R. China and*
[2]*Optical Nanostructures Laboratory, Columbia University, New York, NY 10027, USA*
(Dated: March 13, 2013)

This Supplementary Material is organized as follows. In Sec. I, we present the linearization of the optomechanical Hamiltonian. Using the quantum master equation, we describe the covariance approach to calculate the mean phonon number in Sec. II. With this approach, we derive the steady-state cooling limit in Sec. III and the time evolution of mean phonon number in Sec. IV. In Sec. V, we calculate the instantaneous-state cooling limit in the strong coupling regime and optimize the result according to the frequency matching condition. In Sec. VI, the dynamic modulation of cavity dissipation is introduced. In Sec. VII, we discuss the dissipation quantum backaction and interaction quantum backaction. In Sec. VIII we investigate the effect of dissipation pulsewidth. The discussion on the bad-cavity limit is studied in Sec. IX.

I. LINEARIZED OPTOMECHANICAL HAMILTONIAN

The optomechanical Hamiltonian with one optical mode coupled to one mechanical mode is given by [1]

$$H=-\Delta a^{\dagger}a+\omega_{\rm m}b^{\dagger}b+ga^{\dagger}a(b+b^{\dagger})+(\Omega a^{\dagger}+\Omega^{*}a), \tag{1}$$

where we work in the frame rotating at the input laser frequency ω. Here $\Delta=\omega-\omega_{\rm c}$ is the input-cavity detuning, a (b) is the annihilation operator of the optical (mechanical) mode with $\omega_{\rm c}$ ($\omega_{\rm m}$) being the corresponding angular resonance frequency; g represents the single-photon optomechanical coupling rate; $\Omega=\sqrt{\kappa_{\rm ex}P/(\hbar\omega)}e^{i\phi}$ denotes the driving strength, where P is the input laser power, ϕ is the initial phase of the input laser and $\kappa_{\rm ex}$ is the input-cavity coupling rate.

The quantum Langevin equations are given by

$$\dot{a}=\left(i\Delta-\frac{\kappa}{2}\right)a-iga(b+b^{\dagger})-i\Omega-\sqrt{\kappa_{\rm ex}}a_{\rm in,ex}-\sqrt{\kappa_0}a_{\rm in,0}, \tag{2a}$$

$$\dot{b}=\left(-i\omega_{\rm m}-\frac{\gamma}{2}\right)b-iga^{\dagger}a-\sqrt{\gamma}b_{\rm in}, \tag{2b}$$

where κ_0 is the intrinsic cavity dissipation rate; $\kappa=\kappa_0+\kappa_{\rm ex}$ is the total cavity dissipation rate; γ is the dissipation rate of the mechanical mode; $a_{\rm in,0}$, $a_{\rm in,ex}$ and $b_{\rm in}$ are the noise operators associated with the intrinsic cavity dissipation, external cavity dissipation (input-cavity coupling) and mechanical dissipation, respectively.

Coherent laser input results in the displacements of both the optical and mechanical harmonic oscillators. For convenience, a displacement transformation is applied, i. e., $a\equiv a_1+\alpha$, $b\equiv b_1+\beta$, where α and β are c-numbers, denoting the displacements of the optical and mechanical modes; a_1 and b_1 are the displaced operators, representing the quantum fluctuations of the optical and mechanical modes around their classical values. By separating the classical and quantum components, the quantum Langevin equations are rewritten as

$$\dot{\alpha}=\left(i\Delta'-\frac{\kappa}{2}\right)\alpha-i\Omega, \tag{3a}$$

$$\dot{\beta}=\left(-i\omega_{\rm m}-\frac{\gamma}{2}\right)\beta-ig\left|\alpha\right|^{2}, \tag{3b}$$

$$\dot{a}_1=\left(i\Delta'-\frac{\kappa}{2}\right)a_1-ig\alpha(b_1+b_1^{\dagger})-iga_1(b_1+b_1^{\dagger})-\sqrt{\kappa_{\rm ex}}a_{\rm in,ex}-\sqrt{\kappa_0}a_{\rm in,0}, \tag{3c}$$

$$\dot{b}_1=\left(-i\omega_{\rm m}-\frac{\gamma}{2}\right)b_1-ig\left(\alpha^{*}a_1+\alpha a_1^{\dagger}\right)-iga_1^{\dagger}a_1-\sqrt{\gamma}b_{\rm in}, \tag{3d}$$

*Electronic address: yfxiao@pku.edu.cn; URL: www.phy.pku.edu.cn/∼yfxiao/index.html
†Electronic address: cww2014@columbia.edu

where the optomechanical-coupling modified detuning $\Delta' = \Delta - g(\beta + \beta^*)$. Under strong driving condition, the classical components dominate and the nonlinear terms $iga_1(b_1 + b_1^\dagger)$ and $iga_1^\dagger a_1$ in Eqs. (3c) and (3d) can be neglected, respectively. Then we obtain the linearized Hamiltonian $H_L = -\Delta' a_1^\dagger a_1 + \omega_{\rm m} b_1^\dagger b_1 + (Ga_1^\dagger + G^* a_1)(b_1 + b_1^\dagger)$ (Eq. (1) of the main text), where $G = \alpha g$ is the linearized optomechanical coupling strength.

II. CALCULATION OF MEAN PHONON NUMBER

With the linearized Hamiltonian, the quantum master equation reads

$$\begin{aligned}\dot{\rho} = {} & i[\rho, -\Delta' a_1^\dagger a_1 + \omega_{\rm m} b_1^\dagger b_1 + (Ga_1^\dagger + G^* a_1)(b_1 + b_1^\dagger)] \\ & + \frac{\kappa}{2}\left(2a_1\rho a_1^\dagger - a_1^\dagger a_1\rho - \rho a_1^\dagger a_1\right) + \frac{\gamma}{2}(n_{\rm th}+1)\left(2b_1\rho b_1^\dagger - b_1^\dagger b_1\rho - \rho b_1^\dagger b_1\right) + \frac{\gamma}{2}n_{\rm th}\left(2b_1^\dagger\rho b_1 - b_1 b_1^\dagger\rho - \rho b_1 b_1^\dagger\right), \end{aligned} \tag{4}$$

where $n_{\rm th}$ is the thermal phonon number in the environment. Since the Hamiltonian is linear, it does not mix moments with different orders. To calculate the mean phonon number, it is not necessary to calculate all the matrix elements of the density operator ρ, instead we need to determine the mean values of all the second-order moments, $\bar{N}_a = \langle a_1^\dagger a_1\rangle$, $\bar{N}_b = \langle b_1^\dagger b_1\rangle$, $\langle a_1^\dagger b_1\rangle$, $\langle a_1 b_1\rangle$, $\langle a_1^2\rangle$ and $\langle b_1^2\rangle$. The differential equations are given by

$$\frac{d}{dt}\bar{N}_a = -i\left(G\langle a_1^\dagger b_1\rangle - G^*\langle a_1^\dagger b_1\rangle^* + G\langle a_1 b_1\rangle^* - G^*\langle a_1 b_1\rangle\right) - \kappa\bar{N}_a, \tag{5a}$$

$$\frac{d}{dt}\bar{N}_b = -i\left(-G\langle a_1^\dagger b_1\rangle + G^*\langle a_1^\dagger b_1\rangle^* + G\langle a_1 b_1\rangle^* - G^*\langle a_1 b_1\rangle\right) - \gamma\bar{N}_b + \gamma n_{\rm th}, \tag{5b}$$

$$\frac{d}{dt}\langle a_1^\dagger b_1\rangle = [-i(\Delta + \omega_{\rm m}) - \frac{\kappa+\gamma}{2}]\langle a_1^\dagger b_1\rangle - i\left(G^*\bar{N}_a - G^*\bar{N}_b + G\langle a_1^2\rangle^* - G^*\langle b_1^2\rangle\right), \tag{5c}$$

$$\frac{d}{dt}\langle a_1 b_1\rangle = [i(\Delta - \omega_{\rm m}) - \frac{\kappa+\gamma}{2}]\langle a_1 b_1\rangle - i\left(G\bar{N}_a + G\bar{N}_b + G + G^*\langle a_1^2\rangle + G\langle b_1^2\rangle\right), \tag{5d}$$

$$\frac{d}{dt}\langle a_1^2\rangle = (2i\Delta - \kappa)\langle a_1^2\rangle - 2iG\left(\langle a_1 b_1\rangle + \langle a_1^\dagger b_1\rangle^*\right), \tag{5e}$$

$$\frac{d}{dt}\langle b_1^2\rangle = (-2i\omega_{\rm m} - \gamma)\langle b_1^2\rangle - 2i\left(G^*\langle a_1 b_1\rangle + G\langle a_1^\dagger b_1\rangle\right). \tag{5f}$$

These equations can also be found in Ref. [2], where the steady-state covariance matrix is used to obtain the final occupancy of the mechanical resonator. Note that in the above calculation, cut-off of the density matrix is not necessary and the solutions are exact.

III. STEADY-STATE COOLING LIMIT

In the stable regime, which requires $|G|^2 < -(4\Delta'^2 + \kappa^2)\omega_{\rm m}/(16\Delta')$ for red detuning $\Delta' < 0$ [3], the system finally reaches the steady state, and the derivatives in Eq. (5) all become zero. Then the second-order moments in the steady state satisfy a set of algebraic equations. Under the condition $\Delta' = -\omega_{\rm m}$ and cooperativity $C \equiv 4|G|^2/(\gamma\kappa) \gg 1$, we obtain the final phonon occupancy

$$\bar{N}_{\rm std} \simeq \frac{4|G|^2 + \kappa^2}{4|G|^2(\kappa+\gamma)}\gamma n_{\rm th} + \frac{4\omega_{\rm m}^2\left(\kappa^2 + 8|G|^2\right) + \kappa^2\left(\kappa^2 - 8|G|^2\right)}{16\omega_{\rm m}^2(4\omega_{\rm m}^2 + \kappa^2 - 16|G|^2)}. \tag{6}$$

Here the first term, being proportional to the environmental thermal phonon number $n_{\rm th}$, is the classical cooling limit; the second term, which does not depend on $n_{\rm th}$, corresponds to the quantum cooling limit. In the resolved sideband case, Eq. (6) reduces to Eq. (2) of the main text. Note that Ref. [2] and Ref. [4] present similar results in the strong coupling regime, with the quantum cooling limit $|G|^2/(2\omega_{\rm m}^2)$. In our calculations we find that the term $\omega_{\rm m}^2 - 4|G|^2$ in the denominator cannot be simplified to be $\omega_{\rm m}^2$ for relatively strong coupling strength $|G|$. Therefore, a more exact quantum cooling limit is $|G|^2/[2(\omega_{\rm m}^2 - 4|G|^2)]$, which also indicates that the stable condition $2|G| < \omega_{\rm m}$ should be satisfied.

IV. TIME EVOLUTION OF MEAN PHONON NUMBER

The steady-state solutions do not provide full information of the cooling process. Here we directly solve the differential equations Eq. (5) to obtain the time evolution of mean phonon number. For arbitrary parameters, Eq. (5) can be solved numerically. Especially, under the conditions (1) resolved sideband, (2) $\Delta' = -\omega_{\rm m}$, (3) $C \gg 1$, simple analytical expressions are available for the weak coupling and strong coupling regimes. In the weak coupling regime, using the approximation $\sqrt{16\left|G\right|^2-\kappa^2} \simeq i\kappa$, we obtain

$$\bar{N}_b^{\rm wk} \simeq \frac{(\gamma+\Gamma e^{-\Gamma t})}{\gamma+\Gamma} n_{\rm th} + \frac{\kappa^2}{16\omega_{\rm m}^2}\left(1-e^{-\Gamma t}\right), \tag{7}$$

where $\Gamma = 4|G|^2/\kappa$ is the cooling rate. In this case the cooling process corresponds to the exponential decay (with cooling rate Γ) of the mean phonon number from $n_{\rm th}$ to the steady-state cooling limit $\bar{N}_{\rm std}^{\rm wk} \simeq \gamma n_{\rm th}/(\Gamma+\gamma)+\kappa^2/(16\omega_{\rm m}^2)$.

In the strong coupling regime, to obtain analytical results, it is more convenient to calculate the contribution of the rotating-wave terms $Ga_1^\dagger b_1 + G^* a_1 b_1^\dagger$ and counter-rotating-wave terms $Ga_1^\dagger b_1^\dagger + G^* a_1 b_1$ separately. First, in Eq. (5) the counter-rotating interactions are neglected, then the mean phonon number is obtained as

$$\bar{N}_{b,1}^{\rm str} \simeq n_{\rm th}\frac{\gamma+\frac{1}{2}e^{-\frac{\kappa+\gamma}{2}t}\left[\kappa-\gamma+(\kappa+\gamma)\cos(\omega_+-\omega_-)t\right]}{\kappa+\gamma}, \tag{8}$$

where

$$\omega_\pm = \sqrt{\omega_{\rm m}^2 \pm 2\left|G\right|\omega_{\rm m}} \tag{9}$$

are the eigenfrequencies of the normal modes. This term $\bar{N}_{b,1}^{\rm str}$ is proportional to the environmental thermal phonon number $n_{\rm th}$ and behaves as a decaying Rabi oscillation, corresponding to the beam-splitter interaction $a_1^\dagger b_1 + a_1 b_1^\dagger$. Next, taking the counter-rotating terms into account and setting $n_{\rm th} = 0$, we obtain the contribution of quantum backaction as

$$\bar{N}_{b,2}^{\rm str} \simeq \frac{\left|G\right|^2\left[1-e^{-\frac{\kappa+\gamma}{2}t}\cos(\omega_++\omega_-)t\cos(\omega_+-\omega_-)t\right]}{2(\omega_{\rm m}^2-4\left|G\right|^2)}. \tag{10}$$

Note that $\bar{N}_{b,2}^{\rm str}$ does not depend on $n_{\rm th}$, corresponding to the vacuum fluctuation-induced heating. For $t\to\infty$, $\bar{N}_{b,2}^{\rm str} \to \left|G\right|^2/[2(\omega_{\rm m}^2-4\left|G\right|^2)]$, which is just the steady-state quantum cooling limit. With Eqs. (8) and (10), the time evolution of the mean phonon number in the strong coupling regime is given by $\bar{N}_b^{\rm str} = \bar{N}_{b,1}^{\rm str} + \bar{N}_{b,2}^{\rm str}$ (Eq. (3) of the main text).

V. INSTANTANEOUS-STATE COOLING LIMIT AND FREQUENCY MATCHING

The minimum value of $\bar{N}_{b,1}^{\rm str}$ is obtained when $t \simeq \pi/(\omega_+-\omega_-)$ (half Rabi oscillation cycle), yielding $\cos(\omega_+-\omega_-)t \simeq -1$ and

$$\bar{N}_{b,1}^{\rm str}\,|_{\rm min} \simeq \frac{\gamma n_{\rm th}}{\kappa}\left(1-e^{-\frac{\kappa+\gamma}{2}\frac{\pi}{\omega_+-\omega_-}}\right) \simeq \frac{\pi\gamma n_{\rm th}}{4\left|G\right|}. \tag{11}$$

The minimum value of $\bar{N}_{b,2}^{\rm str}$ depends on the carrier-envelope frequency matching, where the carrier frequency is $\omega_+ + \omega_-$ and the envelope frequency is $\omega_+ - \omega_-$. The frequency matching condition is

$$\frac{\omega_+ + \omega_-}{\omega_+ - \omega_-} = k, \tag{12}$$

where $k = 3, 5...$ In this case when $t = \pi/(\omega_+ - \omega_-)$, we have $\cos(\omega_+ + \omega_-)t = \cos k\pi = -1$, and

$$\bar{N}_{b,2}^{\rm str}\,|_{\rm min}^{\rm opt} \simeq \frac{\left|G\right|^2}{2(\omega_{\rm m}^2-4\left|G\right|^2)}\left(1-e^{-\frac{\kappa+\gamma}{2}\frac{\pi}{\omega_+-\omega_-}}\right) \simeq \frac{\pi\kappa|G|}{8(\omega_{\rm m}^2-4|G|^2)}. \tag{13}$$

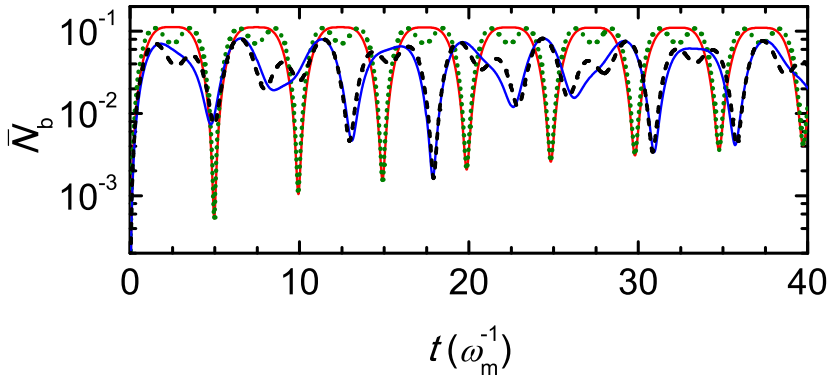

FIG. S1: (color online) (a) Time evolution of $\bar{N}_b$ for $n_{\rm th}=0$, $G/\omega_{\rm m}=0.25$ (black dashed curve) and 0.3 (green dotted curve). The blue and red solid curves are the corresponding analytical results given by Eq. (10). Other parameters are $\kappa/\omega_{\rm m}=0.003$ and $\gamma/\omega_{\rm m}=10^{-5}$.

If the frequency matching condition Eq. (12) is not satisfied, The minimum value of $\bar{N}_{b,2}^{\rm str}$ is obtained when $t\simeq 2\pi/(\omega_+ +\omega_-)$, which yields $\cos(\omega_+ +\omega_-)t\simeq 1$, and

$$\cos(\omega_+ -\omega_-)t\simeq\cos 2\pi\frac{\omega_+ -\omega_-}{\omega_+ +\omega_-}\simeq 1-2(\pi\frac{\omega_+ -\omega_-}{\omega_+ +\omega_-})^2\simeq 1-\frac{2\pi^2|G|^2}{\omega_{\rm m}^2-|G|^2}. \tag{14}$$

Thus we obtain

$$\bar{N}_{b,2}^{\rm str}|_{\rm min}\simeq\frac{|G|^2}{2(\omega_{\rm m}^2-4\,|G|^2)}\times\frac{2\pi^2|G|^2}{\omega_{\rm m}^2-|G|^2}=\frac{\pi^2\,|G|^4}{(\omega_{\rm m}^2-|G|^2)(\omega_{\rm m}^2-4\,|G|^2)}. \tag{15}$$

In the main text, the instantaneous-state cooling limits Eqs. (4) and (5) are from the above expressions.

To verify the optimized instantaneous-state cooling limit, in Fig. S1 we plot the time evolution of phonon occupation starting from $n_{\rm th}=0$ for $G/\omega_{\rm m}=0.25$ and 0.3. It shows explicitly that when $G/\omega_{\rm m}=0.3$, the carrier-envelope frequencies match, leading to minimum phonon occupancy less than 10^{-3}; while without matching ($G/\omega_{\rm m}=0.25$) the minimum phonon number is still 10^{-2} at the first Rabi oscillation cycle. We note that the numerical results agree well with the analytical expressions.

VI. DYNAMIC MODULATION OF CAVITY DISSIPATION

In the above calculations, all the parameters are time-independent. Now we introduce time-dependent cavity dissipation $\kappa(t)$. In this case the master equation (4) and the differential equations (5) still hold. We numerically solve Eqs. (5) to obtain the cooling dynamics, with the main results presented in the main text.

During the modulation of cavity dissipation $\kappa(t)$, we have assumed that the intracavity field α and thus the coupling strength G keeps time-invariant. This can be satisfied by simultaneously modulating the driving strength $\Omega(t)$. From Eqs. (3a) and (3b) we observe that this requires

$$\frac{\Omega(t)}{\Omega(0)}=\frac{i\left(\Delta'+\frac{2|G|^2}{\omega_{\rm m}}\right)-\frac{\kappa(t)}{2}}{i\left(\Delta'+\frac{2|G|^2}{\omega_{\rm m}}\right)-\frac{\kappa(0)}{2}}. \tag{16}$$

Using $\Omega(t)=\sqrt{\kappa_{\rm ex}(t)P(t)/(\hbar\omega)}e^{i\phi(t)}$ the condition reads

$$\sqrt{\frac{\kappa_{\rm ex}(t)P(t)}{\kappa_{\rm ex}(0)P(0)}}e^{i[\phi(t)-\phi(0)]}=\frac{i\left(\Delta'+\frac{2|G|^2}{\omega_{\rm m}}\right)-\frac{\kappa(t)}{2}}{i\left(\Delta'+\frac{2|G|^2}{\omega_{\rm m}}\right)-\frac{\kappa(0)}{2}}. \tag{17}$$

Note that in Eqs. (5) only the total cavity dissipation $\kappa(t)$ appear explicitly. In principle both the modulation of the internal cavity dissipation $\kappa_0(t)$ and the external cavity dissipation $\kappa_{\rm ex}(t)$ leads to the same results as long as Eq. (17) is satisfied. The difference is that the modulation of $\kappa_{\rm ex}(t)$ also changes the light intensity coupled into the cavity.

VII. DISSIPATION QUANTUM BACKACTION AND INTERACTION QUANTUM BACKACTION

In the strong coupling regime, quantum backaction behaves quite different from that in the weak coupling regime. This is because in these two regimes the dominant quantum backaction has distinct origins. In the weak coupling regime, the dominant quantum backaction stems from the added noise which accompanies with the system dissipation, which is a fundamental consequence of the fluctuation-dissipation theorem. This dissipation quantum backaction (DQBA) results in the quantum cooling limit $\kappa^2/(16\omega_{\rm m}^2)$. However, in the strong coupling regime, since the optomechanical interaction dominates over the cavity dissipation, the major contribution is the interaction quantum backaction (IQBA), which leads to the final phonon occupancy $|G|^2/[2(\omega_{\rm m}^2-4|G|^2)]$.

The IQBA is a result of strong counter-rotating interaction. For convenience, let us transform to the normal mode basis, with the relation

$$\begin{pmatrix} a_1 \\ b_1 \\ a_1^\dagger \\ b_1^\dagger \end{pmatrix} = \begin{pmatrix} \eta_{++} & \eta_{-+} & \eta_{+-} & \eta_{--} \\ \eta_{++} & -\eta_{-+} & \eta_{+-} & -\eta_{--} \\ \eta_{+-} & \eta_{--} & \eta_{++} & \eta_{-+} \\ \eta_{+-} & -\eta_{--} & \eta_{++} & -\eta_{-+} \end{pmatrix} \begin{pmatrix} c_+ \\ c_- \\ c_+^\dagger \\ c_-^\dagger \end{pmatrix}, \tag{18}$$

where $c_\pm$ are the eigenmodes with the corresponding eigenfrequencies $\omega_\pm = \sqrt{\omega_{\rm m}^2 \pm 2|G|\omega_{\rm m}}$, and the coefficients

$$\eta_{++} = \frac{1}{2\sqrt{2}}\left(\sqrt{\frac{\omega_{\rm m}}{\omega_+}} + \sqrt{\frac{\omega_+}{\omega_{\rm m}}}\right), \tag{19a}$$

$$\eta_{+-} = \frac{1}{2\sqrt{2}}\left(\sqrt{\frac{\omega_{\rm m}}{\omega_+}} - \sqrt{\frac{\omega_+}{\omega_{\rm m}}}\right), \tag{19b}$$

$$\eta_{-+} = \frac{1}{2\sqrt{2}}\left(\sqrt{\frac{\omega_{\rm m}}{\omega_-}} + \sqrt{\frac{\omega_-}{\omega_{\rm m}}}\right), \tag{19c}$$

$$\eta_{--} = \frac{1}{2\sqrt{2}}\left(\sqrt{\frac{\omega_{\rm m}}{\omega_-}} - \sqrt{\frac{\omega_-}{\omega_{\rm m}}}\right). \tag{19d}$$

It is clear that due to the counter-rotating interaction, the annihilation operators of the eigenmodes are mixtures of the annihilation operators and creation operators of the photon and phonon modes. The degree of mixing is characterized by η_{+-} and η_{--}. A large interaction strength $|G|$ leads to large mode splitting and thereby results in a strong degree of mixing. The final phonon occupancy is roughly proportional to $\eta_{+-}^2+\eta_{--}^2$, which scale as $|G|^2/\omega_{\rm m}^2$.

VIII. EFFECT OF DISSIPATION PULSEWIDTH

The dissipation pulse suppresses the IQBA, while the DQBA is enhanced due to added noise accompanying with the increased dissipation. Thus it is important to optimize the pulse duration. In Fig. S2 we plot the time evolution of mean phonon number under single-pulse modulation with different pulsewidths $T_{\rm p}=0.1T_{\rm R}$, $T_{\rm R}$, $5T_{\rm R}$ and infinity, where $T_{\rm R}=\pi/(2|G|)$ is the half Rabi oscillation cycle. The parameters are the same as that in Figs. 2(c) and (d) of the main text except for the pulsewidths. It shows that within the pulse duration, the phonon number increases gradually, which is the effect of dissipation quantum backaction. To analyze this explicitly, let us consider the case of an infinitely-long dissipation pulse applied from $t=0$, which corresponds to highly unresolved sideband case with cavity dissipation $\kappa_{\rm inf} \gg \omega_{\rm m}$. Using the quantum noise approach, the rate for absorbing and emitting a phonon by the cavity field are respectively given by

$$A_- = \frac{G^2\kappa_{\rm inf}}{\left(\omega_{\rm m}+\Delta'\right)^2+\left(\frac{\kappa_{\rm inf}}{2}\right)^2}, \tag{20a}$$

$$A_+ = \frac{G^2\kappa_{\rm inf}}{\left(\omega_{\rm m}-\Delta'\right)^2+\left(\frac{\kappa_{\rm inf}}{2}\right)^2}. \tag{20b}$$

With detuning $\Delta'=-\omega_{\rm m}$, the net optical damping rate is given by

$$\begin{aligned}\Gamma_{\rm inf} = A_- - A_+ &= \frac{4G^2}{\kappa_{\rm inf}} - \frac{G^2\kappa_{\rm inf}}{\left(2\omega_{\rm m}\right)^2+\left(\frac{\kappa_{\rm inf}}{2}\right)^2} \\ &\simeq \frac{4G^2}{\kappa_{\rm inf}}\left(\frac{4\omega_{\rm m}}{\kappa_{\rm inf}}\right)^2 = \frac{C\gamma}{R},\end{aligned} \tag{21}$$

where we have introduced the resolved sideband parameter $R \equiv \kappa_{\rm inf}^2/(16\omega_{\rm m}^2)$. The final phonon occupancy is calculated as

$$n_{\rm inf} = n_{\rm inf}^{\rm c} + n_{\rm inf}^{\rm q}, \tag{22a}$$

$$n_{\rm inf}^{\rm c} = \frac{\gamma n_{\rm th}}{\gamma + \Gamma_{\rm inf}} \simeq \frac{R n_{\rm th}}{R + C}, \tag{22b}$$

$$n_{\rm inf}^{\rm q} = \frac{A_+}{\gamma + \Gamma_{\rm inf}} \simeq \frac{RC}{R + C} = \frac{4G^2\kappa_{\rm inf}^2}{64G^2\omega_{\rm m}^2 + \gamma\kappa_{\rm inf}^3}. \tag{22c}$$

Note that the results in the resolved sideband (RSB) case are different, which read [5, 6]

$$A_-^{\rm RSB} \simeq \frac{4G^2}{\kappa} = C\gamma, \tag{23a}$$

$$A_+^{\rm RSB} \simeq \frac{G^2\kappa}{4{\omega_{\rm m}}^2} = RC\gamma, \tag{23b}$$

$$\Gamma_{\rm RSB} \simeq \frac{4G^2}{\kappa} = C\gamma, \tag{23c}$$

$$n_{\rm RSB} = n_{\rm RSB}^{\rm c} + n_{\rm RSB}^{\rm q}, \tag{23d}$$

$$n_{\rm RSB}^{\rm c} \simeq \frac{\gamma n_{\rm th}}{\Gamma_{\rm RSB}} \simeq \frac{n_{\rm th}}{C}, \tag{23e}$$

$$n_{\rm RSB}^{\rm q} \simeq \frac{A_+}{\Gamma_{\rm RSB}} \simeq R. \tag{23f}$$

Here $A_-^{\rm RSB} \gg A_+^{\rm RSB}$, thus $A_+^{\rm RSB}$ can be neglected, resulting in the large net optical damping rate $\Gamma_{\rm RSB}$. However, for

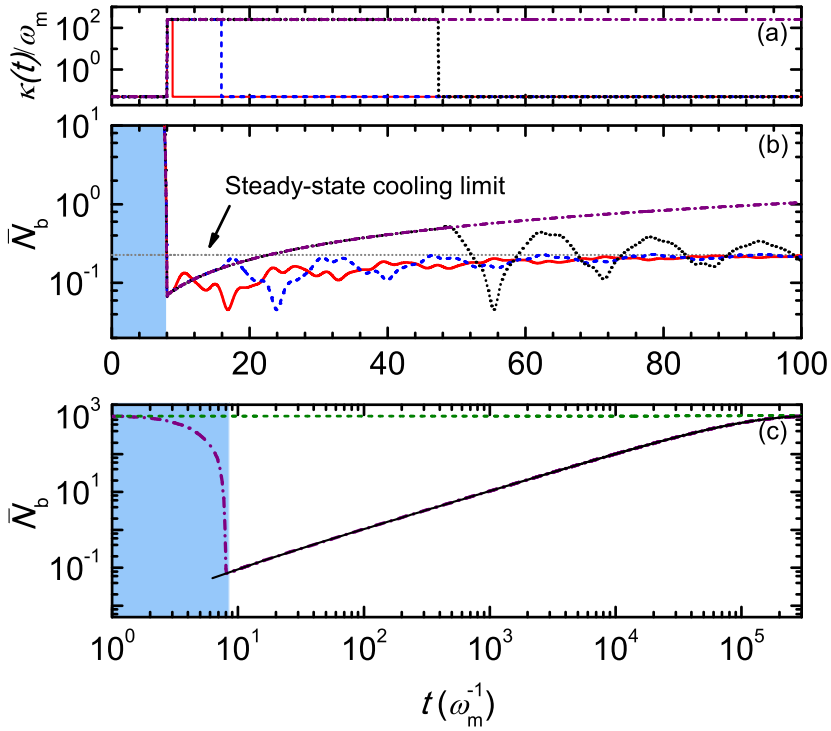

FIG. S2: (color online) (a) Modulation scheme of the cavity dissipation and (b) time evolution of mean phonon number $\bar{N}_b$ under single-pulse modulation for pulsewidth: $0.1T_{\rm R}$ (red solid curve), $T_{\rm R}$ (blue dashed curve), $5T_{\rm R}$ (black dotted curve), infinity (purple dashed-dotted curve). In (b), the dotted horizontal line corresponds to the steady-state cooling limit; the vertical coordinate range from 10 to 10^3 is not shown. (c) Logarithmic-logarithmic plot of $\bar{N}_b$ under single-pulse modulation with infinitely-long pulsewidth applied at $t = T_{\rm R}$ (purple dashed-dotted curve). The black solid curve denotes the analytical results given by Eq. (24) with $n(T_{\rm R}) = 0.07$. The green dashed curve is a comparison with infinitely-long dissipation pulse applied from $t = 0$. Other parameters: $n_{\rm th} = 10^3$, $\gamma/\omega_{\rm m} = 10^{-5}$, $\kappa/\omega_{\rm m} = 0.05$, $G/\omega_{\rm m} = 0.2$.

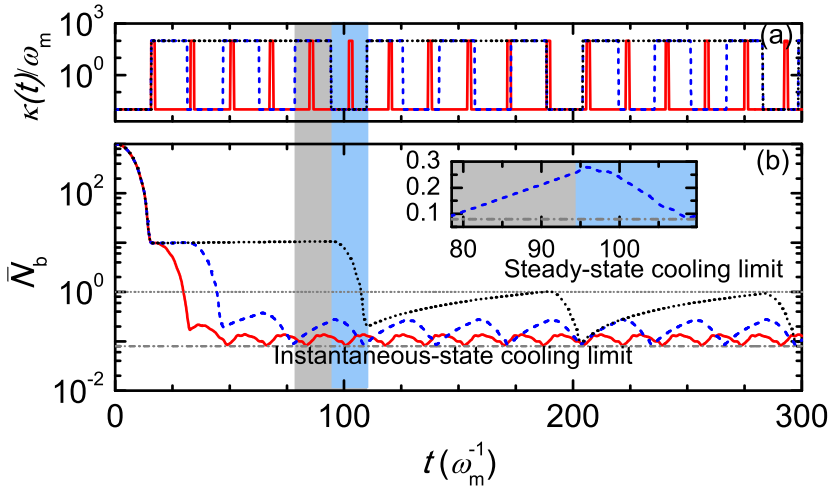

FIG. S3: (color online) (a) Modulation scheme of the cavity dissipation and (b) time evolution of mean phonon number $\bar{N}_b$ under periodic modulation for pulsewidth: $0.1T_R$ (red solid curve), T_R (blue dashed curve), $5T_R$ (black dotted curve). In (b), the dotted (dashed-dotted) horizontal line corresponds to the steady-state (instantaneous-state) cooling limit. The inset is a zoom in linear vertical coordinate view of the shaded region in (b) for T_R pulsewidth, where the gray shaded region illustrates the region of high dissipation (and high dissipation backaction) while the blue shaded region is that of low dissipation. The non-monotonic decay in the blue shaded region is due to residual interaction backaction. Other parameters: $n_{th} = 10^3$, $\gamma/\omega_m = 10^{-5}$, $\kappa/\omega_m = 0.01$, $G/\omega_m = 0.1$.

the highly unresolved sideband case, A_- and A_+ are nearly equal, leading to a small net optical damping rate Γ_{inf}. Furthermore, when calculating the final phonon occupancy, the intrinsic mechanical damping rate γ is negligible in the resolved sideband limit since $\Gamma_{RSB} \gg \gamma$. But in the highly unresolved sideband limit γ cannot be neglected since it could even be larger than the net optical damping rate Γ_{inf}. Considering a specific example, $n_{th} = 10^3$, $\gamma/\omega_m = 10^{-5}$, $\kappa_{inf}/\omega_m = 250$, $G/\omega_m = 0.2$, we obtain $C = 64$, $R = 3906$, yielding $\Gamma_{inf}/\gamma = 0.016$, $n_{inf}^c = 984$, $n_{inf}^q = 63$ and $n_{inf} = 1047$.

We are interested in the time evolution of the mean phonon number with given phonon occupancy at $t = t_0$ in this highly unresolved sideband regime. With the above results, we obtain

$$n(t) = n(t_0) + [n_{inf} - n(t_0)]\left[1 - e^{-(\gamma+\Gamma_{inf})(t-t_0)}\right], \tag{24}$$

$$\frac{dn(t)}{dt} = (\gamma + \Gamma_{inf})\,[n_{inf} - n(t_0)]\,e^{-(\gamma+\Gamma_{inf})(t-t_0)}. \tag{25}$$

For short time scales near $t = t_0$, we have $e^{-(\gamma+\Gamma_{inf})(t-t_0)} \simeq 1$, and $dn(t)/dt \simeq (\gamma+\Gamma_{inf})\,[n_{inf} - n(t_0)]$, which is limited by the small net optical damping rate Γ_{inf}.

In Fig. S2 (c) we plot the time evolution of the mean phonon number under a single infinitely-long dissipation pulse applied at $t = T_R$ (purple dashed-dotted curve). This corresponds to the case that the system is in the highly unresolved sideband regime from $t = T_R$. For comparison, the highly unresolved sideband case starting from $t = 0$ (green dashed curve) is also presented. It shows that, during the pulse duration, the mean phonon number increase exponentially and finally reaches the cooling limit given by Eq. (22). However, the time scale is very large due to the small total damping rate. The analytical expression given by Eq. (24) (black solid curve) is in good accordance with the numerical results. Therefore, in this highly unresolved sideband regime, since the cooling and heating have almost balanced effects, the optical field pose only insignificant effect to the mechanical resonator. When the system has been already cooled to a low-phonon-number state, it will cost a long time (compared with the pulsewidth) for the system to recover to the thermal equilibrium state.

In Fig. S3 we plot the time evolution of mean phonon number under periodic modulation with different pulsewidths $T_p = 0.1T_R$, T_R, $5T_R$. The parameter are the same as that in Fig. 3 of the main text except for the pulsewidth. It is clear that longer pulsewidth leads to the increase of the phonon number, and shorting the pulse will suppress this heating induced by the dissipation quantum backaction arising from fluctuation-dissipation. In the inset, we illustrate a zoom in view for T_R pulsewidth, where the gray (blue) shaded region illustrates the mean phonon number at the region of high (low) dissipation. With pulsewidth $T_p = 0.1T_R$ or shorter, this effect has negligible influence.

IX. DISCUSSION ON THE BAD-CAVITY LIMIT

The dynamic dissipative cooling scheme works in the strong coupling regime ($2|G| > \kappa$). Here we discuss the bad-cavity (unresolved sideband, $\kappa > \omega_{\rm m}$) case. By solving Eq. (5) with all the derivatives being zero, we obtain the generalized version of the steady-state quantum limit which holds both in the good-cavity and bad-cavity conditions

$$\bar{N}_{\rm std}^{\rm q} = \frac{\omega_{\rm m}\left(4\Delta'^2+\kappa^2\right)\left[4\left(\Delta'+\omega_{\rm m}\right)^2+\kappa^2\right]-8G^2\Delta'\left(4\Delta'^2+\kappa^2+16\Delta'\omega_{\rm m}+8\omega_{\rm m}^2\right)}{-16\Delta'\omega_{\rm m}\left[16\Delta'|G|^2+\omega_{\rm m}(4\Delta'^2+\kappa^2)\right]}, \tag{26}$$

where we have used the approximation of small mechanical decay rates γ with respect to ($\omega_{\rm m}$, κ, Δ', $|G|$).

For red detuning $\Delta' < 0$, the dynamical stability condition calculated from the Routh-Hurwitz criterion [3] is given by

$$16\Delta'|G|^2+\omega_{\rm m}(4\Delta'^2+\kappa^2) > 0, \tag{27}$$

which is also embodied in the denominator of Eq. (26). In the unresolved sideband regime, the optimal detuning to achieve the minimum fundamental cooling limit is $\Delta' = -\kappa/2$ [5, 6]. In this case Eq. (27) reduces to

$$|G| < \frac{\sqrt{\kappa\omega_{\rm m}}}{2}, \tag{28}$$

which does not satisfy the strong coupling condition. If we set $\Delta' = -\omega_{\rm m}$, the stable region requires

$$|G| < \sqrt{\frac{\omega_{\rm m}^2}{4}+\frac{\kappa^2}{16}}, \tag{29}$$

which is almost always in the weak coupling regime. One way to avoid this is to use a large detuning $\Delta' \gg \kappa$, then the stable condition reduces to

$$|G| < \frac{\sqrt{|\Delta'|\,\omega_{\rm m}}}{2}. \tag{30}$$

If $|\Delta'| > \kappa^2/\omega_{\rm m}$, strong coupling is a possibility. But in this case the detuning is so large that the cooling efficiency is very low. Therefore, in the bad-cavity limit the dynamic dissipative cooling scheme does not show special advantage.

[1] C. K. Law, Phys. Rev. A **51**, 2537 (1995).
[2] I. Wilson-Rae, N. Nooshi, J. Dobrindt, T. J. Kippenberg and W. Zwerger, New J. Phys. **10**, 095007 (2008).
[3] R. Ghobadi, A. R. Bahrampour, and C. Simon, Phys. Rev. A **84**, 033846 (2011).
[4] J. M. Dobrindt, I. Wilson-Rae, and T. J. Kippenberg, Phys. Rev. Lett. **101**, 263602 (2008).
[5] I. Wilson-Rae, N. Nooshi, W. Zwerger, and T. J. Kippenberg, Phys. Rev. Lett. **99**, 093901 (2007).
[6] F. Marquardt, J. P. Chen, A. A. Clerk, and S. M. Girvin, Phys. Rev. Lett. **99**, 093902 (2007).